JACS
JOURNAL OF THE AMERICAN CHEMICAL SOCIETY
Article
pubs.acs.org/JACS

X-ray Crystal Structure of *rac*-[Ru(phen)$_2$dppz]$^{2+}$ with d(ATGCAT)$_2$ Shows Enantiomer Orientations and Water Ordering

James P. Hall,[†,§] Daniel Cook,[†] Sara Ruiz Morte,[†] Patrick McIntyre,[†] Katrin Buchner,[†] Hanna Beer,[†] David J. Cardin,[†] John A. Brazier,[‡] Graeme Winter,[§] John M. Kelly,[∥] and Christine J. Cardin*[,†]

[†]Chemistry Department, and [‡]Reading School of Pharmacy, University of Reading, Whiteknights, Reading RG6 6AD, United Kingdom

[§]Diamond Light Source, Didcot, Oxfordshire OX11 0DE, United Kingdom

[∥]School of Chemistry, Trinity College, Dublin 2, Ireland

Supporting Information

ABSTRACT: We report an atomic resolution X-ray crystal structure containing both enantiomers of *rac*-[Ru(phen)$_2$dppz]$^{2+}$ with the d(ATGCAT)$_2$ DNA duplex (phen = phenanthroline; dppz = dipyridophenazine). The first example of any enantiomeric pair crystallized with a DNA duplex shows different orientations of the Λ and Δ binding sites, separated by a clearly defined structured water monolayer. Job plots show that the same species is present in solution. Each enantiomer is bound at a TG/CA step and shows intercalation from the minor groove. One water molecule is directly located on one phenazine N atom in the Δ-enantiomer only.

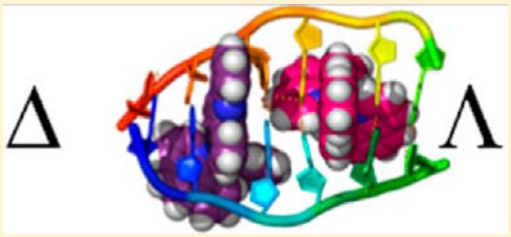

INTRODUCTION

The interaction of metal complexes with DNA is an area that has been of biomedical importance since Rosenberg's original finding that cisplatin causes *E. coli* bacteria to stop dividing and instead elongate 300-fold.[1] The field now encompasses a wide range of platinum, rhodium, ruthenium, and other metal complexes,[2,3] including two ruthenium complexes that reached clinical trials.[4,5] Precise experimental data showing how these complexes interact with DNA targets remain rare, because of the difficulty of crystallization. When available, such studies provide a wealth of information unobtainable any other way. Here, we report not only the first structure showing how the ruthenium "light-switch" complex Δ-[Ru(phen)$_2$dppz]$^{2+}$ (**1**) (phen = phenanthroline; dppz = dipyridophenazine) binds to DNA, but also the first example of how any enantiomeric pair recognizes a DNA duplex. This is a fascinating study, because the inherent right-handed chirality of DNA is necessarily accommodated in different ways by the two enantiomers, as was originally pointed out for the [Ru(phen)$_3$]$^{2+}$ cations.[6]

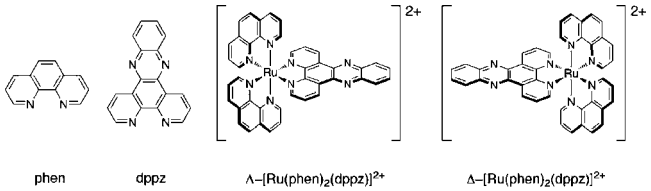

1

The Λ- and Δ-enantiomers of **1** are one of an important group of synthetic metallointercalators.[7] These complexes have been extensively studied as biosensors[8] and therapeutic agents,[9] and can be incorporated into living cells. The "light-switch" property refers to the luminescence of the compound when bound to DNA or in aprotic solvents such as acetonitrile, but not in aqueous solution. This behavior was initially studied using the racemic compound, and later the resolved enantiomers.[10] In a classic study, Hiort, Lincoln, and Norden first developed a method for preparing the pure enantiomers.[11] They then showed that both enantiomers are bound to calf thymus DNA with binding constants of about 10^8 M^{-1} in low ionic strength buffer. Their careful work showed that, despite this similarity, the relative luminescence quantum yield of the bound Δ-enantiomer was 6−10 times larger than that of the bound Λ-enantiomer. Our own recent work has suggested that the two lifetimes may also be correlated with symmetrical and angled intercalation,[12] which is in agreement with the latest data from their ongoing studies.[13] In the intervening period, there has been much discussion about the meaning of the results, although the measurements are not in dispute. The main assumption has been that the emission lifetimes must be related to the extent to which water is excluded from the dppz by the intercalation into DNA.[14] Two excited-state lifetimes were observed even with a single enantiomer and homopolymer, with variations in the proportions of the two lifetimes depending on the loading of the DNA. It follows therefore that different lifetimes should correlate with different orientations and intercalation depths of the dppz chromophore, and a number of binding models have been proposed.[15,16]

We recently obtained the first crystal structures showing two intercalation modes for the Λ-enantiomer of **1**.[12] A symmetric

Received: April 10, 2013
Published: July 23, 2013

   dx.doi.org/10.1021/ja403590e | J. Am. Chem. Soc. 2013, 135, 12652−12659

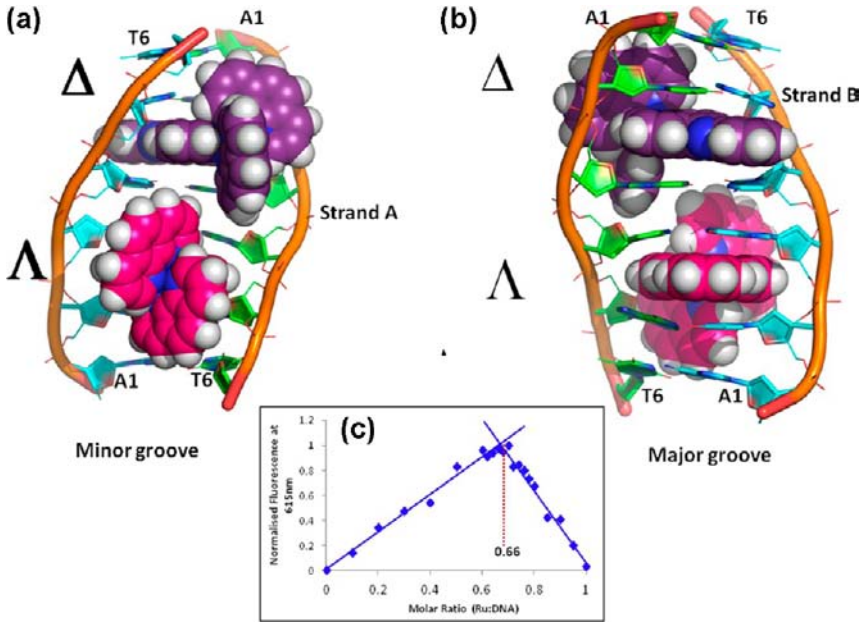

Figure 1. Assembly of the duplex. (a) View into the minor groove. Nucleotides of d(ATGCAT) strand A are colored green, and those of strand B are in cyan. The Δ-enantiomer of **1** is purple, and the Λ-enantiomer is pink. Both enantiomers are intercalated so that a phen ligand stacks against a nucleoside sugar, Δ against T_2 of strand A, and Λ against A_5 of strand A. (b) View into the major groove, oriented to look down the long axis of the dppz ligand of the Λ-enantiomer. (Figures were drawn with PyMol.) (c) Fluorescence Job plot, showing maximum normalized fluorescence in solution at the stoichiometric ratio corresponding to the structure in (a) and (b). For the absorption spectra, see Figure S1, and for more fluorescence data, see Figure 5.

perpendicular intercalation from the minor groove was seen at the central TA/TA step in the duplex d(CCGGTACCGG)$_2$, and an angled intercalation, also from the minor groove, at the terminal GG/CC step. It seems plausible to correlate these two binding modes with the two photochemical lifetimes, as done by Lincoln.[13] Their data require the assignment of the shorter lifetime to the symmetric intercalation mode, which is plausible, because our study showed a greater accessibility to the dppz chromophore in this orientation. What remains puzzling about the crystallization is the complete enantiomeric specificity observed, starting with the racemic compound in the crystallization solution. Although exclusively incorporated into the crystal lattice, the Λ-enantiomer has been shown by numerous studies to be more weakly bound in solution.[10] A possible reason is that semi-intercalation[17] by one of the two phen ligands in the minor groove causes the crystal packing generated to be enantiospecific. The use of a second sequence, d(CCGGATCCGG), reversing the central step, resulted in no incorporation of either enantiomer at that site, perhaps for steric reasons. We have therefore sought other systems, which might enable the well-documented Δ-binding to be directly observed. The recent crystallographic study from the Barton laboratory shows the Δ-enantiomer of $[Ru(bpy)_2dppz]^{2+}$ intercalated from the minor groove at CG/CG and AT/AT steps,[18] as part of a study of mismatch recognition. Binding to mismatched adenine−adenine resulted in flipping out of the adenine and stacking with an adjacent bpy ligand in the minor groove. In agreement with our own observations, there is some sequence specificity in the orientation of the dppz chromophore, with a nearly symmetrical intercalation direction of 82° at the AT/AT step, but here the depth of intercalation is restricted by the adenine stacking in the minor groove.

We now report the first structure showing both enantiomers of **1**, here bound to a single d(ATGCAT)$_2$ duplex. This hexameric duplex has never previously been crystallized, either alone or with a bound ligand. It shows an unexpected interaction between two angled intercalators, both bound at the TG/CA steps of the duplex, and thus together, recognizing the 5′-TGCA-3′ sequence. The phen ligands are dovetailed, interleaved by a single water layer, in a highly ordered minor groove. The intercalation is not at the terminal steps; thus the resulting model may well be applicable to solution data, with the Λ- and Δ-enantiomers indeed having different orientations in their intercalation cavities.

RESULTS

Although the d(ATGCAT) self-complementary sequence used in this work has never been crystallized before, it has been used in two NMR studies of bisintercalation.[19,20] In those cases, the bisintercalating aromatic charged chromophore was inserted at the TG/CA steps with the flexible linker in the major groove. These authors found a strong specific binding in solution at pH 7 and 15 °C, with specific NMR signals still detectable at 25 °C, and with protonation of a phenazine N in the intercalation cavity.

Racemic $[Ru(phen)_2(dppz)]Cl_2$ and the hexamer d(ATGCAT), in a buffer containing spermine, 2-methyl-2,4-pentanediol, sodium cacodylate pH 7.0, NaCl, and $BaCl_2$ were allowed to stand in the dark at 20 °C. Crystals formed after a few weeks as orange needles. The crystals were flash-frozen, and their structure was subsequently characterized by X-ray crystallography (data measured at 100 K). Full details of the data collection and refinement statistics are given in the Methods, and Table S1, with the full conformational analysis in Table S2. We have attempted to crystallize the pure enantiomers separately with the same hexamer, but so far have not been successful, suggesting that this may be a very unusual case of enantiomeric cooperative binding.

dx.doi.org/10.1021/ja403590e | J. Am. Chem. Soc. 2013, 135, 12652−12659

Description of the Structure. The self-complementary duplex crystallized in a trigonal lattice, with an asymmetric unit consisting of two DNA strands, A and B, and one each of the Λ- and Δ-enantiomers of $[Ru(phen)_2dppz]^{2+}$ (**1**), as shown in Figure 1a and b. (Figure 1c is a Job plot showing that the same stoichiometric binding ratio is present in solution.) Details of the packing are shown in Figure S2. The conformation is an overall B-type DNA, but with a low overall twist (sum of the five twist angles is only 116°), probably due to the steric requirements of the phen ligands in the minor groove.

The Intercalation Cavities. Both Λ- and Δ-enantiomers of **1** are intercalated from the minor groove at the TG/CA steps of the duplex. The Δ-enantiomer is bound at T_2-G_3(A)/C_4-A_5(B), and the Λ-enantiomer at T_2-G_3(B)/C_4-A_5(A). The two cavities have somewhat different geometries, but what is immediately striking is that both enantiomers are packed against strand A. The Δ-enantiomer packs against T_2(A), whereas the Λ-enantiomer packs against A_5(A).

Figure 2 shows the two intercalation cavities, seen from both sides, showing the Δ-enantiomer to be more acutely angled, at

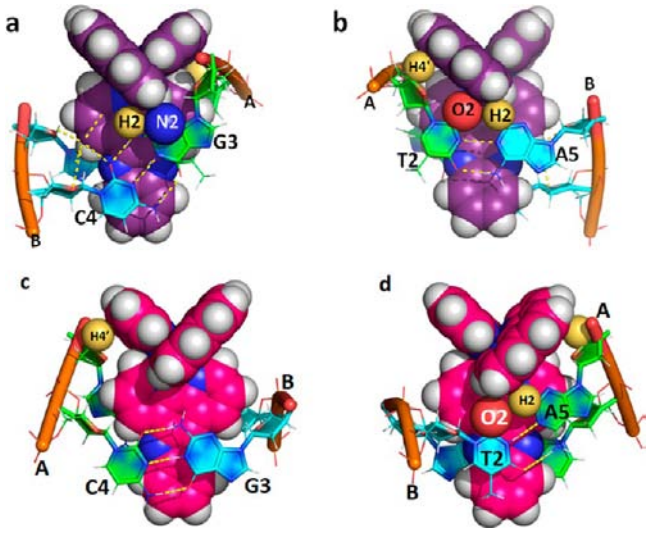

Figure 2. The Δ- and Λ-enantiomer intercalation cavities. Both enantiomers are shown in projections from both sides, with contact atoms from the nucleic acid component labeled. (a) The Δ-enantiomer from the G_3(A)-C_4(B) side. The phen ligand makes a close contact with the 2-NH_2 group of G_3(A). (b) The Δ-enantiomer from the T_2(A)-A_5(B) side. The second phen ligand makes a close contact with H4′ and O2 of T_2(A), and with H2 of A_5(B). (c) The Λ-enantiomer from the C_4(A)-G_3(B) side. In contrast to (a), the Λ-enantiomer makes no close contacts with the C_4(A)-G_3(B) basepair. The H4′ contact visible is to the H4′ of A_5(A). (d) The Λ-enantiomer from the A_5(A)-T_2(B) side. There are close contacts to O2 of T_2(B) and to H2 of A_5(A), as in (b), but the angle of intercalation is less acute, and the contacts to a Λ-oriented phen ligand.

65°, with the Λ-enantiomer almost perpendicularly, but not symmetrically, intercalated, at 87°. The P−P separation vector is used to define the intercalation angle of the duplex, the distances here being 16.6 Å for Δ and 16.0 Å for Λ, with the angle defined relative to the dppz long axis (Figure 3). Other distinctive geometrical parameters are the local twist angles, with the Δ-enantiomer higher, at 30.0°, as compared to the unexpectedly low Λ-enantiomer value at 22.2°.

The differently angled enantiomers give rise to a much more favorable Ru−P orientation and distance in the Δ-enantiomer (Table 1). Here, the closest Ru−P distance is only 6.8 Å (to strand A), as compared to a shortest Ru−P distance of 8.6 Å for the Λ-enantiomer (to strand B), suggesting a possible origin for the known stronger binding of the Δ-enantiomer in solution.[10] The shorter separation is combined with a more favorable alignment, shown in Figure 3 (Ru−P vectors shown as purple dotted lines), with only the Δ-enantiomer aligned along the approximate bisector of the Ru−N vectors and orthogonal to the long axis of the dppz ligand. Further details of the structure are shown in Figures S2−S5.

As intercalation is from the minor groove, it might be expected that the 2-NH_2 group of guanine might be a dominant feature determining the depth of intercalation. Comparison of Figure 2a and c shows that, while this may be correct for the Δ-enantiomer (Figure 2a; N2 and H2 contacts shown as spheres), it is not the case for the Λ-enantiomer (Figure 2c). Here, the C_4(A)-G_3(B) basepair is stacked over the phenazine ring of the dppz ligand, remote from any phen contacts. The AT basepair does, however, make contact with each enantiomer (Figure 2b and d). In both cases, the thymine oxygen O2 and the adenine hydrogen C−H2 are the contact atoms, although at different angles due to the differently angled chromophores. While the Λ intercalation geometry could be described as head-on (perpendicular), it is not symmetric, because of the asymmetric nature of the intercalation site.

Water Organization. The structure contains 96 fully occupied water positions, with only a small solvent channel. Most of the water is directly bound to the DNA phosphate oxygen atoms and to the bases in the grooves. Figure 4a shows a view into the major groove. Both enantiomers have a chain of water molecules across the C11−C12 (end) face of the dppz ligand, but with one exception there is no other water interaction with dppz. In the minor groove, there is extensive ordering around the phen ligands, particularly between strand B of the duplex and the ligands.

Figure 4b highlights the exceptional case. Because of the more acute intercalation angle of the Δ-enantiomer, combined with the somewhat greater depth of intercalation, one face of the dppz ligand of the Δ-enantiomer is more exposed in the major groove, whereas the other is less exposed (Figure 6, see discussion). Here, a directly bound water molecule can be seen in a fully occupied site on the dppz phenazine N atom in Figure 4b. Although the Λ-enantiomer has both faces of the dppz ligand exposed, neither binds ordered water, although there will obviously be disordered water, even in the "frozen glass" environment of the crystal structure. To understand this difference, it is necessary to examine the ordering role of the G3 carbonyl groups in the major groove. The orientation of the Δ-enantiomer has this carbonyl group aligned to form part of the H-bond network shown in Figure 4b. For the Λ-enantiomer, the local environment is hydrophobic on both faces of the dppz ligand, as shown in Figure 4a and c. For this enantiomer, although both phenazine nitrogen atoms are exposed, it is to disordered water.

Conformational Switching at the Intercalation Cavities. Figure 5a and b shows the two enantiomer intercalation cavities viewed directly into the cavities along the long axes of the dppz ligand. The overall shapes of the two cavities show curvature chiefly associated with one strand only. In the case of the Λ-enantiomer, this is strand B, while for the Δ-enantiomer, it is strand A. In both cases, the parallel stacking is associated with the T_2-G_3 sequence. It is also associated with the adoption of an overall extended conformation of the DNA backbone on

dx.doi.org/10.1021/ja403590e | J. Am. Chem. Soc. 2013, 135, 12652−12659

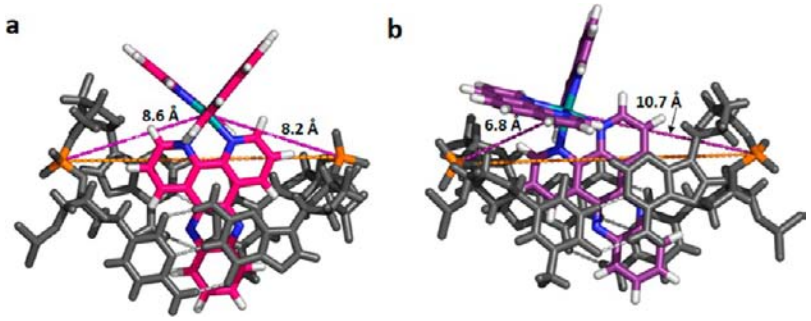

Figure 3. Chromophore orientation. (a) Λ and (b) Δ orientations of the two enantiomers used to define the data in Table 1.

Table 1

	Λ	Δ
Nucleic Acid Parameters		
local helical rise (Å)	6.7	6.9
local helical twist (deg)	22. 7	30.3
P−P separation (Å)	16.0	16.6
Ligand Parameters		
Ru−N distance (mean) (Å)	2.1	2.1
angle between Ru−N square plane and dppz plane (deg)	10.6	11.6
Intercalation into the TG/CA Site		
Phen ligand contacts on strand A	Ade 5	Thy 2
intercalation angle (deg)	87	65
Ru−P closest approach (Å)	8.6 (on strand B)	6.8 (on strand A)

this side of the intercalation cavity. The normal B-DNA structure has a synclinal (sc) rotamer around the exocyclic C4′−C5′ bond of the 2′-deoxyribose sugar, determining the normal orientation of the phosphate relative to the sugar ring, and measured by the γ torsion angle of the backbone. In this structure, both G_3 residues have the antiperiplanar (ap) rotamer, with γ torsion angles of −178° on strand A and +174° on strand B. This rotamer is sometimes found associated with intercalation.[21] Here, it is important because the rotamer switch brings the phosphate closer to the ruthenium atom than in the alternate conformation, and the electrostatic attraction may be the driving force for the switch. What is also evident is that the P−P vectors across the cavity (shown with orange dashes) are not coincident with the dppz ligand planes, perhaps also due to the switch, but entirely consistent with the model of Lincoln et al.,[22] which deduced an alignment of about +15° for both enantiomers.

Solution Measurements. We have also carried out experiments to determine whether the observed simultaneous binding of the two enantiomers might be found for the racemate in solution. We observed the fluorescence melting temperature of the $d(ATGCAT)_2$ duplex in the presence of the

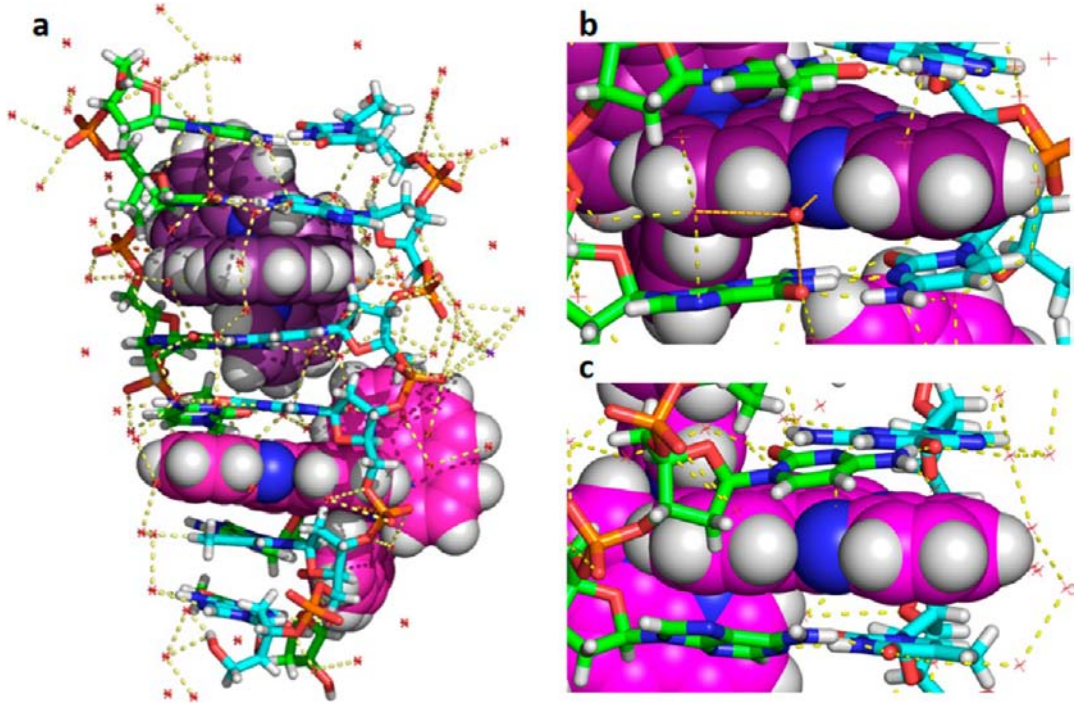

Figure 4. Water organization between the enantiomers. (a) The complete water network. All ordered water is included (red ×) together with the connecting hydrogen bonds (yellow dashes). (b) The Δ-enantiomer, showing the ordered water molecule bound to the dppz N atom. The connectivity of this atom is highlighted as orange dashes. The ordering is facilitated by the proximity of the corbonyl O of G3(A) (see text). (c) The Λ-enantiomer from the corresponding viewpoint. The ordered water network is generated entirely by the DNA bases in the major groove.

dx.doi.org/10.1021/ja403590e | J. Am. Chem. Soc. 2013, 135, 12652−12659

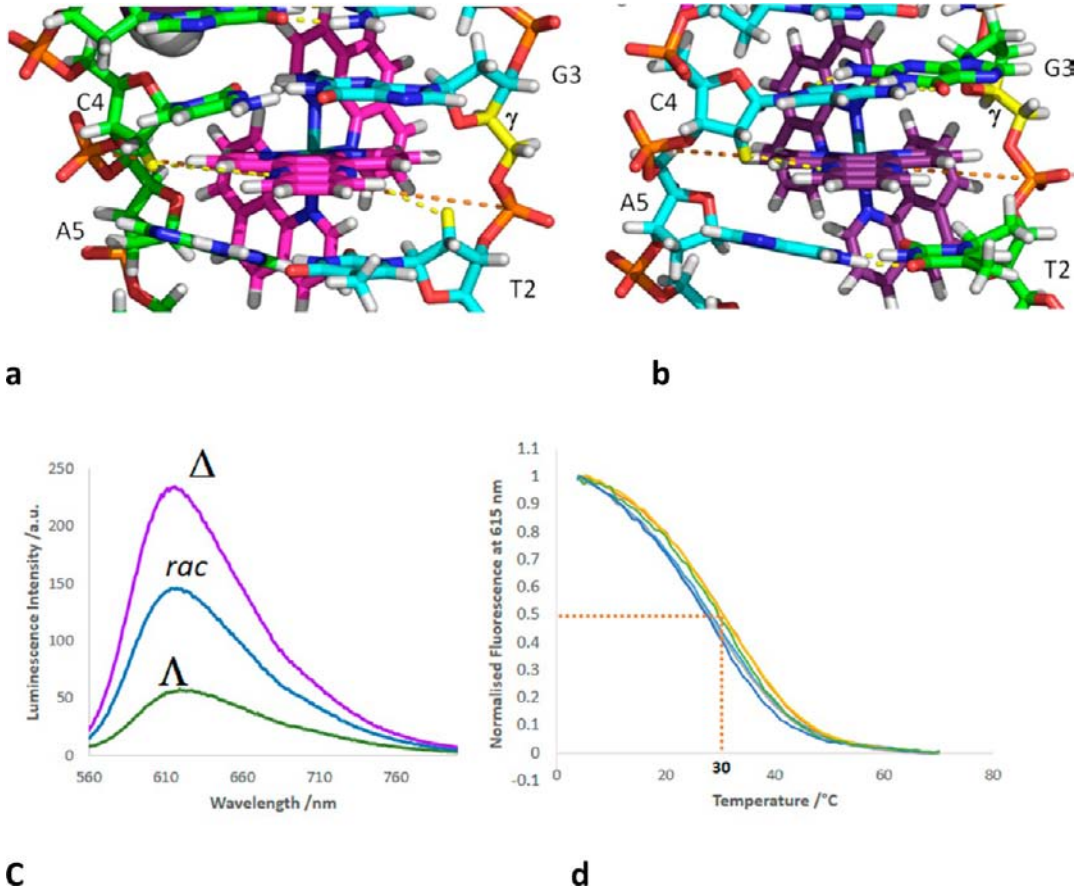

Figure 5. Comparison of the enantiomers. (a) The lambda intercalation cavity looking from the major groove along the dppz ligand plane. (b) The delta intercalation cavity in a similar orientation with respect to the DNA sequence. Strand A is green, and strand B is cyan. All water molecules are removed for clarity. The P−P vectors across both cavities are shown as orange dashed lines. (c) The different fluorescence spectra obtained with the duplex on additions of equimolar amounts of the Δ, Λ, and racemic complexes of **1**, to give in each case a 2 Ru/1 duplex ratio. Purple trace, Δ-enantiomer; blue trace, racemic mixture; green trace, Λ-enantiomer. Excitation at the isosbestic point of 475 nm. (d) Fluorescence melting at the maximum in (c), 615 nm. The heating and cooling traces are almost superimposed, giving a melting temperature of ∼30°.

racemic mixture to be 30° (Figures 5c,d and S1). To determine the binding stoichiometry, luminescence titrations were carried out at 4°, so as to be sure of stable duplex formation. The observed behavior was similar to that seen with high molecular weight DNA in the pioneering studies of Hiort et al.[11] with a linear increase in fluorescence at low Ru:DNA ratios. The stoichiometry was evaluated using the method of continuous variation (Job plot) (Figure 1c), monitoring the optimum stoichiometry of binding using fluorescence at 4°. This gave a maximum at 0.67 (Figure 1c), an indication that in solution the racemic pair binds in a 1:1:1 binding ratio of Λ:Δ:duplex, and consistent with the supramolecular assembly of the crystal structure being found in solution. Corresponding Job plots for the separate Λ- and Δ-enantiomers gave less well-defined Job plot maxima, suggesting that a mixture of 2:1 and 3:1 complexes is formed and not a single species. This suggests that the formation of the interlocked assembly of the crystal structure is a behavior confined to the racemic mixture of enantiomers.

Small Molecule Structures. There are very few small molecule structures available at time of writing in the Cambridge Structural Database showing ruthenium complexes possessing dppz or substituted dppz groups. Perhaps the most relevant to this work is the crystal structure of $[Ru(bpy)_2(6,7\text{-dicyano-dppz})](PF_6)_2$,[23] which shows that the substituted dppz groups stack in the structure with the $dppz(CN)_2$ group from the Λ-enantiomer stacking onto $dppz(CN)_2$ from the Δ. The substituted dppz groups are, at their closest, 3.489(9) Å apart, indicating $\pi-\pi$ stacking. There is little overlap of the bpy groups. The mean Ru−N distance is approximately 2.06 Å, which is in agreement with that observed in the complexes bound to DNA. While we have made attempts to crystallize the racemic-$[Ru(phen)_2(dppz)](PF_6)_2$, no useful data have been obtained so far. The structure of *rac*-$[Ru(phen)_3][PF_6]_2$ is known[24] and shows no stacking of the phenanthroline groups. The Ru−N mean bond length is also 2.06 Å.

■ CONCLUSIONS

This Article reports a very unusual crystal structure in which two enantiomers bind to a short sequence of double-stranded DNA. Of special interest is that the two cations are bound to an (TG/CA) identical step, so that for the first time we are able to directly compare the nature of the binding site, which accommodates each enantiomer. Both enantiomers intercalate from the minor groove side but with very different orientations. Figure 6 sums the similarities and differences. Figure 6 shows that, when the two conformations of the two strands are superimposed, what is most striking is not the differences but the similarities, as was already shown in Figure 5. Between bases T_2 and G_3, the opened backbone is defined by the γ

dx.doi.org/10.1021/ja403590e | J. Am. Chem. Soc. 2013, 135, 12652−12659

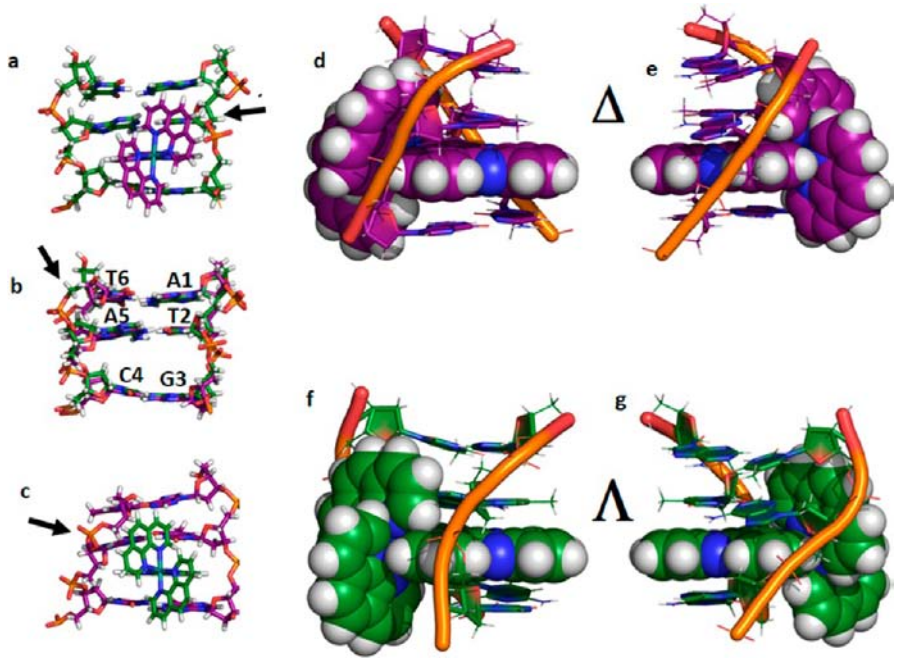

Figure 6. Differences between the Λ- and Δ-enantiomers. (a) The Δ-enantiomer orientation superimposed on the Λ nucleic acid conformation. There would be a clash at residue T_2. (b) The Δ and Λ nucleic acid conformations superimposed using the algorithm in pymol. (c) The Λ-enantiomer conformation superimposed on the Δ nucleic acid conformation. There would be a bad clash with residue A_5, which in the Λ conformation of the nucleic acid is avoided (marked with arrows in (b) and (c)). (d) The Δ conformation seen from the strand A side. There is a fully occupied water position on the phenazine N atom, omitted here for clarity. (e) The Δ conformation seen from the strand B side, in which water access to the phenazine N atom is restricted. (f) The Λ conformation seen from the strand A side. (g) The Λ conformation seen from the strand B side. There is water access to both phenazine N atoms. The two halves of the duplex are here colored green (Λ) and purple (Δ) to highlight the differences between the nucleic acid conformations.

torsion angle of ∼180°, rather than the typical B-DNA value of ∼ +60° seen on the opposing strand. The net effect, therefore, is to highlight that bases T_2 and G_3 are parallel to each of the two dppz chromophores, even though these chromophores are oriented very differently.

In the original discussions about how the two enantiomers might interact with the inherently right-handed B-DNA chain, it was pointed out that the Δ-enantiomer was a better fit, as the Λ-enantiomer would clash with the nucleic acid backbone.[6] The present study shows exactly how this original insight manifests itself at the level of one particular pyrimidine-purine base step, with the comparatively minor adjustments in the conformations of residues T_2 and A_5 but the very different dppz orientations. Figure 6 shows the Δ-enantiomer orientation superimposed on the Λ nucleic acid conformation, with an arrow marking the clash with the deoxyribose sugar of residue T2, which is minimized in the corresponding Δ sugar conformation. There is a bigger clash when the Λ-enantiomer is superimposed on the Δ nucleic acid conformation, with the P atom of residue T6 displaced by 1.2 Å. The orientation of the dppz chromophore is of great importance to an understanding of the differing luminescence behavior of the two enantiomers. In our previous study, which showed both angled and symmetric intercalation of the Λ-enantiomer, at CC/GG and TA/TA DNA steps, respectively, we proposed that the symmetric orientation seen at the TA/TA step was the one that might be associated with a shorter photochemical lifetime. The currently accepted understanding of photochemical lifetime in this system is that the determining factor is water access to the dppz phenazine N atoms. Figure 6d−g examines the four phenazine N atoms seen in this study, and their immediate environments. Figure 6d shows the Δ-enantiomer on the exposed side, which has a water molecule H-bonded at the normal distance of 2.9 Å, already highlighted in Figure 4. By contrast, as shown in Figure 6e, due to the 67° intercalation angle of the Δ-enantiomer, water access to the opposing phenazine N atom must be very limited. Figure 6f and g shows the corresponding views for the Λ-enantiomer, showing that water can readily access both phenazine N atoms. The greater exposure of the Λ-enantiomer to mobile water is due to a combination of the almost perpendicular intercalation and the antiperiplanar conformation at residue G_3.

The picture presented here is thus one in which we are able to see how the two different enantiomers are oriented in the same intercalation cavity. It is inherently an asymmetric mixed sequence cavity and seems to highlight a preference for binding to a pyrimidine-purine step. The Δ-enantiomer has the shorter Ru−P distance (giving a stronger electrostatic attraction) and higher DNA twist angle, an overall more favorable geometry. The Λ-enantiomer has an almost perpendicular geometry, has a longer Ru−P separation, and also has a lower DNA twist angle.

It is intriguing that it is the Δ-enantiomer where there is evidence of an ordered water molecule H-bonded to one of the phenazine N atoms. Given the clear evidence from solution studies that water coordination is responsible for the rapid deactivation of the excited state in the presence of water, this finding would appear to confirm the proposal by Lincoln and other workers that efficient deactivation requires that both phenazine N atoms are in contact with water. In the present structure, it is clear that this is the case for the Λ-enantiomer. The two enantiomers also differ in the precise location of the phenazine N-atoms with respect to the basepairs creating the

dx.doi.org/10.1021/ja403590e | J. Am. Chem. Soc. 2013, 135, 12652−12659

cavity (Figures S3–S5). In the Λ-enantiomer, this atom is sandwiched by the basepairs, but more exposed in its Δ counterpart. In their NMR study of the same $(dATGCAT)_2$ oligonucleotide with a bisphenazine compound, Yang noted that the inserted phenazine was protonated (despite the fact that the pK_a of the molecule in solution was only ca. 1), highlighting the role of charge neutralization, combined with stacking interactions, in stabilizing the conjugate acid form of the phenazine chromophore. As there is no evidence that either of the enantiomers has a protonated ground state in our crystals, we believe that that a facile protonation of the excited state, when between the aromatic rings of bases, could possibly contribute to the much shorter lifetime of the Λ-enantiomer of **1**.

The interaction of racemic **1** with a decamer duplex has previously been studied with the $d(GAG\mathbf{TGCA}CTC)_2$ duplex,[25] which contains the same central **TGCA** sequence. In that experiment, 10 μM **1** mixed with 10 μM $d(GAG\mathbf{TGCA}CTC)_2$ was treated with increasing concentrations of Δ-α-[Rh(*R*,*R*)-Me_2trien]phi]$^{3+}$. A decrease in the emission yield of the ruthenium complex fluorescence showed that the ruthenium complex was being displaced from the DNA stack by the rhodium complex, a result that is quite consistent with the structure seen here, because the rhodium complex is known to bind in the major groove at the central GC/GC step only, and so could not be simultaneously bound with ruthenium at the adjacent step.

In summary, we see here a distinct binding motif for an enantiomeric pair, comprising two intercalations at differing angles, leading to different chromophore orientations in the intercalation cavity. The original intuition that a Δ handed octahedral $M(L-L)_3$ complex must be a better fit to the right-handed DNA duplex is here visualized for the first time, 60 years after the original double helix model was proposed.[26]

METHODS

Synthesis of Complexes. *rac*-[Ru(phen)$_2$(dppz)]·2Cl was synthesized by a literature method.[11] The pure enantiomers were prepared by a modified literature method[11] and characterized by CD spectroscopy and 700 MHz NMR. Full details are available in Supporting Information S1.

Crystallization, Data Collection, and Structure Solution. The oligonucleotide d(ATGCAT) was purchased from ATDBio (Southampton) as a solid purified by double HPLC. The crystallization for 4E87 was performed, using the sitting drop method, using 1 uL of 2 mM d(ATGCAT), 1 uL of 4 mM racemic-[Ru(phen)$_2$(dppz)]·Cl$_2$, and 8 uL of 40 mM sodium cacodylate pH 6.3, 12 mM spermine-HCl, 20 mM $BaCl_2$, 2% 2-methyl-2,4-pentanediol (MPD), and 80 mM NaCl, equilibrated against 1 mL of 35% MPD. Orange rods, approximately 80 × 20 × 20 μm in size, grew in 3–4 weeks at 18 °C.

The data for 4E87 were collected on beamline I04 at Diamond Light Source. 180 images were collected, with a 1° oscillation angle, giving a total of 180° of data. The data were collected using radiation with a wavelength of 1.6531 Å at 100 K. The data were processed using xia2[27−29] with XDS[30−32] giving 3397 unique reflections and an anomalous slope of 1.565.[33] The phasing was determined using FastEP (Diamond Light Source, unpublished) with SHELXC/D/E.[34] Two heavy atoms were located per asymmetric unit and were assigned to both be ruthenium cations with 100% occupancy. The model was built using Coot[35] and refined using Refmac version 5.6[36] from the CCP4[37] suite to give a final R_{cryst} of 0.17 and R_{free} of 0.20 with 5% of reflections reserved for the R_{free} set. The model was deposited in the Protein Data Bank with ID 4E87.

The crystallization for 4JD8 was performed, using the sitting drop method, using 1 uL 2 mM d(ATGCAT), 4 uL of 4 mM racemic [Ru(phen)$_2$(dppz)]·Cl$_2$, and 6 uL of 40 mM sodium cacodylate pH 6.3, 12 mM spermine-HCl, 20 mM $BaCl_2$, 10% 2-methyl-2,4-pentanediol (MPD), and 80 mM KCl equilibrated against 1 mL of 40% MPD. Orange rods, approximately 200 × 50 × 50 μm in size, grew in 2 weeks at 18 °C.

The data for 4JD8 were collected on beamline I02 at Diamond Light Source using radiation with a wavelength of 0.9795 Å at 100 K. 400 images were collected with an oscillation angle of 0.15° to give a total of 60° of data. The data were processed using MOSFLM[38] and Aimless[39] giving 15 894 unique reflections. The structure was solved using molecular replacement with Phaser[40] and the lower resolution model, 4E87. The structure was updated using Coot and refined using Phenix[41] to a final R_{cryst} of 0.13 and R_{free} of 0.16 with 5% of reflections reserved for the R_{free} set. The model was deposited in the Protein Data Bank with ID 4JD8.

For data collection and refinement statistics, see Table S1.

ASSOCIATED CONTENT

Supporting Information

Preparation of complexes, supplementary figures, data collection and refinement statistics, and conformational parameters. This material is available free of charge via the Internet at http://pubs.acs.org.

AUTHOR INFORMATION

Corresponding Author

c.j.cardin@rdg.ac.uk

Notes

The authors declare no competing financial interest.

ACKNOWLEDGMENTS

We thank G. Doorley (formerly of Trinity College Dublin) for preparing the racemic ruthenium complex, and P. Lincoln (Chalmers University, Gothenburg, Sweden) for reading a draft of the manuscript, very helpful discussions, and making available his unpublished observations. J.P.H. is funded by Diamond Light Source and a University of Reading University studentship. D.C. was funded by an EPSRC vacation studentship, S.R.M. by the EU ERASMUS programme, P. McI. by a University of Reading Undergraduate Placement (UROP), and K.B. and H.B. by the EU Leonardo da Vinci mobility programme. We acknowledge additional financial support from the Royal Society, the Royal Irish Academy, and the Science Foundation Ireland (grant 06/RF/CHP035).

REFERENCES

(1) Rosenberg, B.; Van Camp, L.; Krigas, T. *Nature* **1965**, *205*, 698–699.
(2) Komor, A. C.; Barton, J. K. *Chem. Commun.* **2013**, *49*, 3617–3630.
(3) Liu, H.-K.; Sadler, P. J. *Acc. Chem. Res.* **2011**, *44*, 349–359.
(4) Alessio, G.; Mestroni, G.; Bergamo, A.; Sava, C. *Curr. Top. Med. Chem.* **2004**, *4*, 1525–1535.
(5) Hartinger, C. G.; Zorbas-Seifried, A.; Jakupec, M. A.; Kynast, B.; Zorbas, H.; Keppler, B. *J. Inorg. Biochem.* **2006**, *100*, 891–904.
(6) Barton, J. K.; Danishefsky, A. T.; Goldberg, J. M. *J. Am. Chem. Soc.* **1984**, *106*, 2172.
(7) Friedman, A. E.; Chambron, J. C.; Sauvage, J. P.; Turro, N. J.; Barton, J. K. *J. Am. Chem. Soc.* **1990**, *112*, 4960–4962.
(8) Wei, M.-Y.; Guo, L.-H.; Famouri, P. *Microchim. Acta* **2011**, *172*, 247–260.
(9) Yu, H.-J.; Chen, Y.; Yu, L.; Hao, Z.; Zhou, L. *Eur. J. Med. Chem.* **2011**, *55*, 146–154.
(10) Haq, I.; Lincoln, P.; Suh, D.; Norden, B.; Chowdhry, B. Z.; Chaires, J. B. *J. Am. Chem. Soc.* **1995**, *117*, 4788–4796.
(11) Hiort, C.; Lincoln, P.; Nordén, B. *J. Am. Chem. Soc.* **1993**, *115*, 3448–3454.

(12) Niyazi, H.; Hall, J. P.; O'Sullivan, K.; Winter, G.; Sorensen, T.; Kelly, J. M.; Cardin, C. J. *Nat. Chem.* **2012**, *4*, 621−628.
(13) Andersson, J.; Fornander, l.H.; Abrahamsson, M.; Tuite, E.; Nordell, P.; Lincoln, P. *Inorg. Chem.* **2013**, *52*, 1151−1159.
(14) Turro, C.; Bossmann, S. H.; Jenkins, Y.; Barton, J. K.; Turro, N. J. *J. Am. Chem. Soc.* **1995**, *117*, 9026−9032.
(15) Tuite, E.; Lincoln, P.; Norden, B. *J. Am. Chem. Soc.* **1997**, *119*, 239−240.
(16) McKinley, A.; Lincoln, P.; Tuite, E. M. *Coord. Chem. Rev.* **2011**, *255*, 2676−2692.
(17) Hall, J. P.; O'Sullivan, K.; Naseer, A.; Smith, J. A.; Kelly, J. M.; Cardin, C. J. *Proc. Natl. Acad. Sci. U.S.A.* **2011**, *108*, 1761−17614.
(18) Song, H.; Kaiser, J. T.; Barton, J. K. *Nat. Chem.* **2012**, *4*, 615−620.
(19) Dai, J.; Punchihewa, C.; Mistry, P.; Ooi, A. T.; Yang, D. *J. Biol. Chem.* **2004**, *279*, 46096−46103.
(20) Gallego, J.; Read, B. R. *Biochemistry* **1999**, *38*, 15104−15115.
(21) Todd, A. K.; Adams, A.; Thorpe, J. H.; Denny, W. A.; Wakelin, L. P.; Cardin, C. J. *J. Med. Chem.* **1999**, *42*, 536−540.
(22) Lincoln, P.; Broo, A.; Nordén, B. *J. Am. Chem. Soc.* **1996**, *118*, 2644−2653.
(23) Rusanova, J.; Decurtins, S.; Rusanov, E.; Stoeckli-Evans, H.; Delahaye, S.; Hauser, A. *J. Chem. Soc., Dalton Trans.* **2002**, 4318−4320.
(24) Nakamura, A.; Tomohiro, S.; Kuroda, R. *Chem. Commun.* **2004**, 2858−2859.
(25) Holmlin, R. E.; Stemp, E. D. A.; Barton, J. K. *Inorg. Chem.* **1998**, *37*, 29−34.
(26) Watson, J. D.; Crick, F. H. C. *Nature* **1953**, *171*, 737−738.
(27) Winter, G. *J. Appl. Crystallogr.* **2010**, *43*, 186−190.
(28) Sauter, N. K.; Grosse-Kunstleve, R. W.; Adams, P. D. *J. Appl. Crystallogr.* **2004**, *37*, 399−409.
(29) Zhang, Z.; Sauterm, N. K.; Van den Bedem, H.; Snell, G.; Deacon, A. M. *J. Appl. Crystallogr.* **2006**, *39*, 112−119.
(30) Kabsch, W. *J. Appl. Crystallogr.* **1993**, *26*, 795−800.
(31) Kabsch, W. *J. Appl. Crystallogr.* **1988**, *21*, 67−72.
(32) Kabsch, W. *J. Appl. Crystallogr.* **1988**, *21*, 916−924.
(33) Howell, P. L. *J. Appl. Crystallogr.* **1992**, *25*, 81−86.
(34) Sheldrick, G. M. *Acta Crystallogr., Sect. D* **2008**, *64*, 113−122.
(35) Emsley, P.; Lohkamp, B.; Scott, W.; Cowtan. *Acta Crystallogr., Sect. D* **2010**, *66*, 486−501.
(36) Murshudov, G. N.; Vagin, A. A.; Dodson, E. J. *Acta Crystallogr., Sect. D* **1997**, *53*, 240−255.
(37) Collaborative computational project, number 4.. *Acta Crystallogr., Sect. D* **1994**, *50*, 760−763.
(38) Leslie, A. G. W.; Powell, H. R. Evolving Methods for Macromolecular Crystallography. *NATO Science Series*; 2007; Vol. *245*, pp 41−51.
(39) Evans, P. R. *Acta Crystallogr.* **2011**, *D65*, 282−292.
(40) McCoy, A. J.; Grosse-Kunstleve, R. W.; Adams, P. D.; Winn, M. D.; Storoni, L. C.; Read, R. J. *J. Appl. Crystallogr.* **2007**, *40*, 658−674.
(41) Adams, P. D.; Afonine, P. V.; Bunkóczi, G.; Chen, V. B.; Davis, I. W.; Echols, N.; Headd, J. J.; Hung, L.-W.; Kapral, G. J.; Grosse-Kunstleve, R. W.; McCoy, A. J.; Moriarty, N. W.; Oeffner, R.; Read, R. J.; Richardson, D. C.; Richardson, J. S.; Terwilliger, T. C.; Zwart, P. H. *Acta Crystallogr., Sect. D* **2010**, *66*, 213−221.